Table 3 lists the preliminary determinations, computed from preentry tracking data, of entry and impact locations for each of the spacecraft. Flight path angles (fpa) at entry are also shown. These impact locations are also plotted on Fig. 1 superimposed with the corresponding orbit 5. During the more than 2.5 hours of multiprobe mission duration (1824:26 to 2055:34 UT), the orbiter was about 4 to 6.5 hours postperiapsis of orbit 5. With reference to Fig. 2, this period corresponds to altitudes above 40,000 km—that is, geometrically quite close to apoapsis. From Fig. 1, it is clear that the orbiter had good "viewing" of the entry locations for the southern hemisphere probes during the multiprobe mission and good viewing of those for the northern hemisphere probes about 1 to 2 hours prior to periapsis.

Scientific experiments. There are 12 scientific experiments on the orbiter, two on the bus, seven on the large probe, and three identical experiments on each of the smaller north, day, and night probes. In addition, there are several radio-science experiments that make use of the radio systems, either separately or together, on each of the spacecraft. Preliminary results, covering approximately the first 30 days, from most of the experiments are reported in the following papers. The papers are arranged by discipline, from the top of the atmosphere to the surface: solar wind, solar wind-ionosphere interactions, ionosphere, upper atmosphere, remote sensing of the cloud tops, atmosphere structure, cloud structure, thermal balance, atmospheric composition, circulation and dynamics, and surface.

LAWRENCE COLIN
Ames Research Center,
Moffett Field, California 94035

References and Notes

1. For the required background material, see "Venus exploration," *Space Science Reviews* **20**, 248 (May 1977); *ibid.*, pp. 356–525 (June 1977).
2. For a type 2 trajectory, the spacecraft travels more than 180° around the sun; for a type 1 trajectory this angle is less than 180°.
3. Orbit numbers increase by one each time the spacecraft passes through apoapsis. Orbit 0 began at orbit insertion and ended with the first apoapsis, whereupon orbit 1 commenced. The inbound leg of each orbit passes over the northern hemisphere of Venus.
4. Adjustments may also be made at times to periapsis altitudes below 150 km, should atmospheric drag limitations and other considerations permit. In fact, periapsis altitude was reduced to 148 km on orbit 30 (3 January 1979). Current operations provide for weekly corrections to maintain periapsis altitude between 180 and 150 km, at least for the first 100 orbits, a smaller range than the nominal shown in Table 1. Also, infrequent, small orbital period adjustments from the nominal value shown in Table 1 will be made by thruster burns near periapsis to maintain suitable ground tracking station visibility.
5. Definition of 1970 IAU coordinate system for Venus: "For Venus, the origin of planetographic longitudes is defined such that the central meridian of Venus as observed from the center of the Earth is 320.0° at 0^h on 20 June 1964 (Julian Date, 2438566.5). The rotational axis shall be provisionally defined as having a north pole direction of right ascension (α) 273.0° and declination (δ) + 66.0° (1950.0). For the purposes of obtaining longitudes at earlier or later time, a provisional value for the sidereal rotational period of 243.0 days is adopted (from the proceedings of the Fourteenth General Assembly, Brighton 1970, Transactions of the International Astronomical Union, Vol. 14B, Reidel Publishing Co., Holland, 1971)." Based on more recent data, the Pioneer Venus Science Steering Group adopted the IAU convention with a modified north pole direction α = 273.3°, δ = 67.3° (1950.0); see I. I. Shapiro, W. De Campli, D. B. Campbell, *Astrophys. J. Lett.*, in press. A mean value of 6052 km is assumed for the radius of Venus, also.
6. Periapsis occurs within Earth occultation for the first 80 orbits with durations of up to 23 minutes. An apoapsis occultation season occurs between orbits 154 and 164, with longer durations up to 3.5 hours. An occultation radius of 6139.5 km (87.5 km altitude) has been assumed. There are two solar eclipse seasons, orbits 24 to 124 with durations up to 24 minutes and orbits 181 to 188 with duration up to 3.5 hours. An eclipse radius of 6130 km (78 km altitude) has been assumed.
7. Times are at the spacecraft. Ground-received times are larger by one-way light time, 3^m12^s, on this day.
8. I would like to thank the entire Pioneer Venus team, not only C. F. Hall, project manager, and his staff and others at the Ames Research Center, but also other individuals at other NASA centers and industry who helped produce and execute these exceptional and extraordinarily complex missions. In particular, S. Dorfman and his team at the Hughes Aircraft Company, builders of the spacecraft, should be congratulated for providing superb spacecraft performance. Also, R. B. Miller and the staff at the DSN stations should be singled out for their real-time tracking of the multiprobe mission on 9 December 1978. I thank also C. F. Hall, J. W. Dyer, and J. R. Cowley, Jr., for review of this manuscript.

15 January 1979

Initial Pioneer Venus Magnetic Field Results: Dayside Observations

Abstract. *Initial observations by the Pioneer Venus magnetometer in the sunlit ionosphere reveal a dynamic ionosphere, very responsive to external solar wind conditions. The locations of the bow shock and ionosphere are variable. The strength of the magnetic field just outside the ionopause is in approximate pressure balance with the thermal plasma of the ionosphere and changes markedly from day to day in response to changes in solar wind pressure. The field strength in the ionosphere is also variable from day to day. The field is often weak, at most a few gammas, but reaching many tens of gammas for periods of the order of seconds. These field enchantments are interpreted as due to the passage of spacecraft through flux ropes consisting of bundles of twisted field lines surrounded by the ionospheric plasma. The helicity of the flux varies through the flux tube, with low pitch angles on the inside and very large angles in the low-field outer edges of the ropes. These ropes may have external or internal sources. Consistent with previous results, the average position of the bow shock is much closer to the planet than would be expected if the solar wind were completely deflected by the planet. In total, these observations indicate that the solar wind plays a significant role in the physics of the Venus ionosphere.*

This report is a summary of the results obtained by the UCLA fluxgate magnetometer on the first 24 orbits of the Pioneer Venus orbiter. The solar zenith angle of periapsis ranged from an initial 63° to 99° on orbit 24. At the altitude of the spacecraft the ionosphere was sunlit throughout each pass. During these 24 orbits, which included the major part of a solar rotation, there was a wide range of solar wind conditions, resulting in a wide range of ionospheric conditions. The observations reported here were prepared from preliminary digital data relayed daily over telephone lines from Ames Research Center. These records have more data gaps than there will be in the final processed tapes and cover only the region near periapsis. Further, they do not include inertial reference information for the time when the spacecraft is nearest the planet. Thus we have no information at present on the orientation of the magnetic field in the spin plane of the satellite in the ionosphere, and only plots of the magnetic field magnitude will be presented.

Venus has been visited by numerous spacecraft carrying magnetometers. Mariners 2, 5, and 10 flew by at distances ranging from 6.6 to 1.7 Venus radii (R_V). The Venera 4 mother, or bus, spacecraft penetrated the nighttime ionosphere, returning data from altitudes as low as 200 km. Veneras 9 and 10 orbited Venus with 48-hour orbits and 1500-km periapsis altitudes. These earlier missions revealed that Venus has a well-developed bow shock, which deflects and heats the solar wind around the planetary obstacle in much the same way as Earth's bow shock (*1*). The Venus bow shock has much smaller dimensions, however. Verigin *et al.* (*2*) place the nose of the shock at 1.5 R_V; average nose distance of Earth's bow shock is 14 earth radii. Other analyses suggest that the nose position of the shock may be as close to the planet as 1.2R_V, which has been interpreted as implying significant absorption of the

0036-8075/79/0223-0745$00.75/0

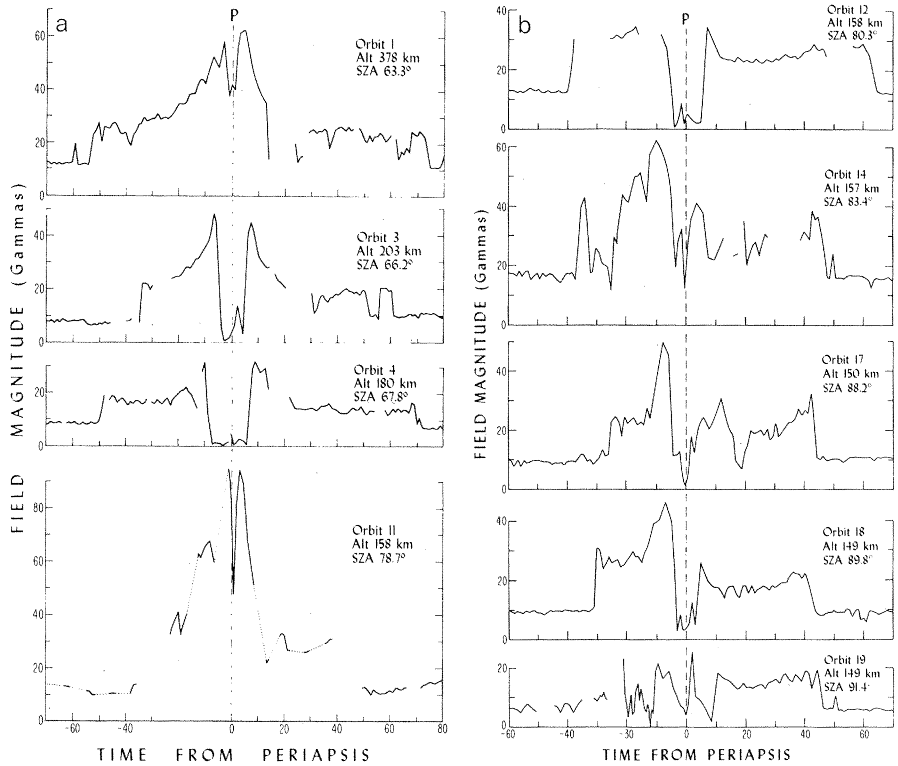

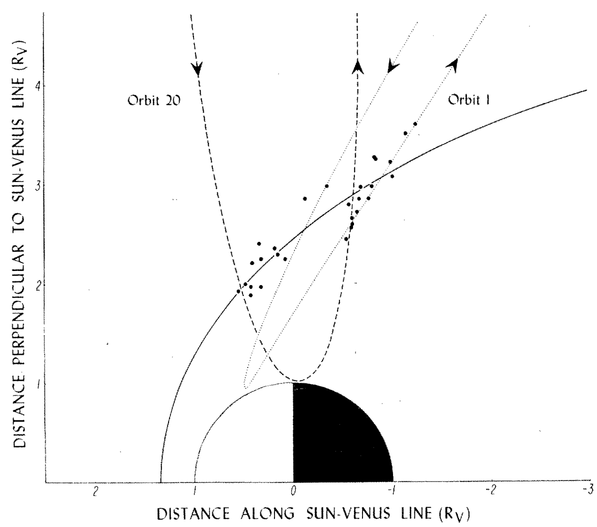

Fig. 1 (above). (a) Average magnetic field strength as a function of time from periapsis for orbits 1, 3, 4, and 11. The altitude (*alt*) and solar zenith angle (*SZA*) at periapsis are also given for each orbit. (b) Average magnetic field strength for orbits 12, 14, 17, 18, and 19. Fig. 2 (left). Positions of bow shock crossings observed on orbits 1 to 24, together with trajectories of orbits 1 and 20. All observations have been rotated into a common plane about the sun-Venus line. The best least-squares fit to these uncorrected data points is shown.

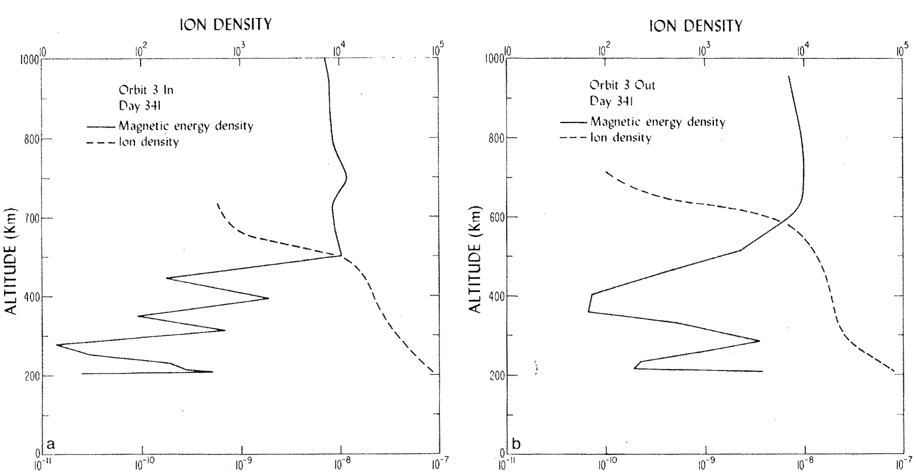

Fig. 3. (a) Altitude variation of 30-second averages of the magnetic field energy density (solid line) and ion density measured by the electron temperature probe (dashed line) on orbit 3 inbound. (b) Altitude variation for orbit 3 outbound.

solar wind by the planetary atmosphere (*3*).

It is clear from the observed location of the bow shock that the planetary ionosphere, and not an intrinsic planetary magnetic field, is the obstacle to the flow of solar wind, in contrast to the situation at Earth and Mercury. Thus, there has been speculation that Venus may not have a magnetic field. On the other hand, there are features in the Mariner 5 and Veneras 4, 9, and 10 data that resemble those expected for a magnetic moment more than 1000 times smaller than that of Earth and with opposite polarity (*4*). The evidence is far from unambiguous.

Pioneer Venus carries new and improved instruments to Venus. It also has the major advantage over previous missions in that its periapsis is deep in the ionosphere. Thus we have been able to probe directly the region in which the solar wind-planetary interaction occurs. Later, when periapsis moves directly behind the planet, we should be able to resolve unambiguously the existence of any intrinsic planetary moment.

Figure 1 shows averages of the measured magnetic field strength through periapsis on nine orbits (*5*). These data were chosen because of the relative completeness of the records. The averaging interval is over two major frames of the telemetry sequence and hence varies with telemetry rate. In Fig. 1 the averaging interval varies from 64 to 128 seconds. Orbit 1 illustrates the major features of the interaction. The satellite first penetrates the bow shock in a series of three multiple crossings, during which the magnetic field is suddenly enhanced. Behind the shock, in the region called the magnetosheath, the field strength continues to rise as the planet is approached, reaching a peak on orbit 1 of about 60 γ (1 $\gamma = 10^{-5}$ gauss). The peak field strength in this region is highly correlated with the solar wind dynamic pressure (*6*) and is in approximate pressure balance with the ionospheric plasma at closer radial distances (*7*).

Closer to periapsis the field strength drops as the spacecraft passes through the ionopause into the ionosphere and rises again upon exit from the ionopause. Back in the magnetosheath, the field strength drops as the spacecraft recedes from the planet, returning abruptly to interplanetary field levels when the satellite crosses the bow shock into the solar wind.

Observations on orbit 3 are similiar to those on orbit 1, except that the field strength in the ionosphere is much lower, often around 1 γ or less. On orbit 4 the field strength just outside the ionosphere reaches only about 30 γ. The field depression coinciding with the ionopause is encountered earlier, and hence at a higher altitude than on the preceding orbit. The exit is also at higher altitudes. These two observations are consistent with a reduced solar wind pressure at this time (*6*). Again, the field strength near periapsis at times is less than 1 γ. Orbit 11, in contrast, has a peak field strength of more than 90 γ, a much lower ionopause altitude, and a high field at periapsis. Orbit 12, one day later, shows how rapidly conditions can change. The ionosphere has returned to its usual dimensions and there is little field enhancement just outside the ionopause. Orbit 14 shows that the solar wind interaction is not always regular. From terrestial experience we would expect this irregularity to be associated with the direction of the interplanetary magnetic field. Orbits 17 and 18 show a marked difference in field strength when the spacecraft enters and leaves the ionopause. This asymmetry is presumably associated with the difference in solar zenith angle of the crossings, the exit being farthest from the sun. Finally, orbit 19 shows a highly irregular magnetosheath, in which the field increase to normal levels does not occur until very near the ionopause. If we associate the low field values with solar wind-type plasma such as occurs in quasi-parallel shocks at Earth (*8*), orbit 19 illustrates how close the solar wind-type plasma can get to the planet. We note that these observations were made close to the terminator region.

The location and shape of the bow shock are important indicators of the nature of the solar wind interaction with the planet. The Venus bow shock has been shown to be closer to Venus than the Mars shock is to Mars (*2*), and this has been interpreted in terms of absorption of the solar wind (*3*). Figure 1 shows that the time relative to periapsis of the bow shock crossings, and hence their location, is quite variable. Figure 2 shows the positions of 29 bow shock crossings observed on orbits 1 to 24, together with the trajectory of the spacecraft on orbits 1 and 20 in this cylindrical coordinate system. The best least-squares fit of a conic section with Venus at the focus for the 29 crossings gives a nose radial distance of 1.32 ± 0.07 R_V and an eccentricity of 0.84 ± 0.07. Because of the orbital motion of Venus the apparent direction of the solar wind is not radially outward from the sun. Using the measured solar wind speed (*6*), we obtain a nose radius of 1.23 ± 0.05 R_V and an eccentricity of 0.92 ± 0.06. Thus, our data support previous estimates of a low nose altitude for the shock. A better measure of the nose distance awaits direct observations in the subsolar region in May 1979.

Figure 3 shows the altitude variation of the magnetic energy density on the inbound and outbound legs of orbit 3. The dashed profile is the ion density measured by the GSFC electron temperature probe. When the pressure is calculated from the measured temperature and density of the ionospheric plasma, there is approximate pressure balance between the external field and the plasma (*7*). Within the ionosphere the 30-second averages of the magnetic energy density show much structure. Although the averaged magnetic energy density in the ionosphere is much less than that just outside it, for short periods of time it can exceed the outside density. In fact, the largest fields encountered to date have been in the ionosphere.

Figure 4 shows the high-resolution data obtained during three intervals on orbit 3: across the inbound ionopause, at periapsis, and across the outbound ionopause. The drop in field strength at the ionopause is abrupt and somewhat irregular; this irregularity is probably associated with motions of the boundary. The unexpected finding in these data is the exceedingly large field strength near periapsis for very brief periods of time. The field strength near periapsis is significantly greater than that just outside the ionopause, but only for a few seconds. In fact, since the instrument is filtered to restrict the bandwidth of the telemetered signals, the true amplitude of these peaks may be even greater.

Although there is no inertial reference information for these data, we know the spin period of the satellite sufficiently well to "despin" the sensors into a reference system with unknown orientation in the spin plane. Examining the three-dimensional nature of the field variation, we find that these features are flux ropes with straight central field lines helically wrapped with lines that diminish in field strength and increase in helical angle with distance from the center of the rope. These flux ropes appear to be similar in many respects to magnetic flux ropes on the sun.

The satellite requires several seconds to cross one of these flux ropes. The strongest and narrowest rope is crossed in 7 seconds, during which the satellite

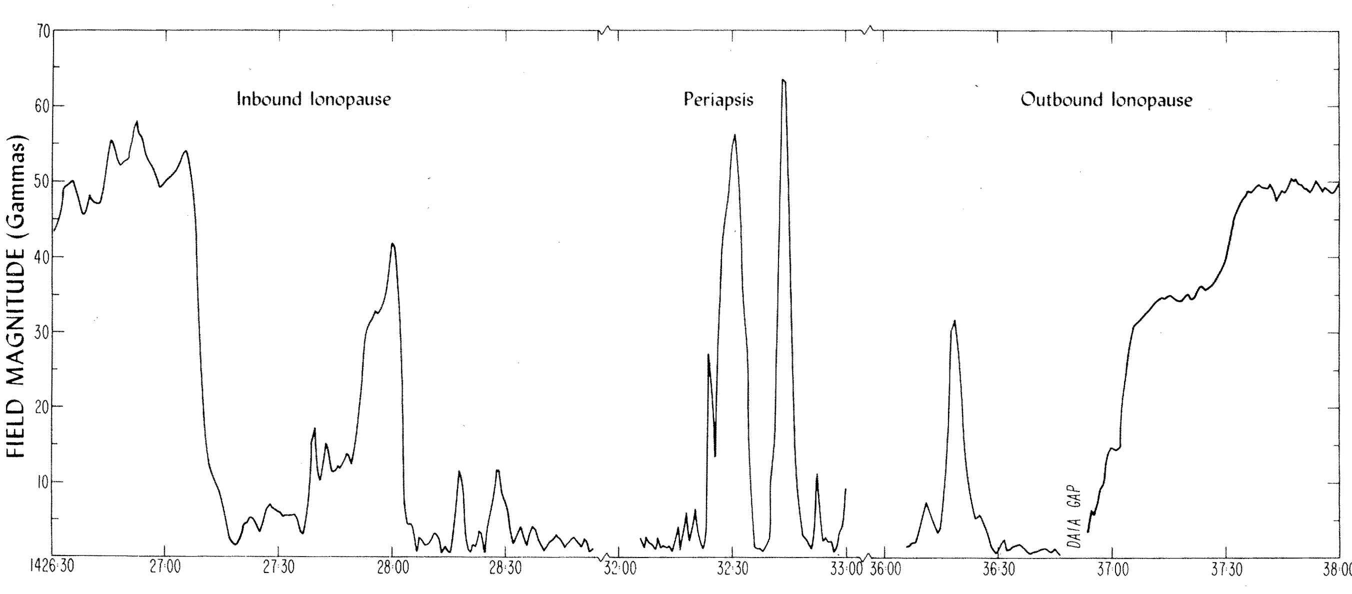

Fig. 4. High-time-resolution magnetic field strength across the inbound and outbound ionopause crossings on orbit 3 and a sample of measurements near periapsis.

has moved 68 km. However, part of this motion may be along the axis of the rope. We obtained a minimum estimate of the diameter of the rope by assuming that it is horizontal and using the altitude variation of the spacecraft; this lower limit is 1.3 km. A better estimate awaits the determination of the relative orientation of the axis of these flux ropes and the satellite trajectory.

The existence of flux ropes in the Venus ionosphere is thus far the major surprise of the magnetic field investigation. At present we can only speculate on the source of these ropes; they could come from either above or below the ionosphere. Perhaps the tension in the field lines draped over the ionopause pulls a flux bundle down deep into the ionosphere. But if so, why are they found so deep in the ionosphere near the terminator region? Perhaps tubes of flux of an intrinsic planetary field are bubbling through the ionosphere on the dayside and being swept back by the ionospheric flow to form a planetary magnetotail. Shears in the flow would twist these tubes into ropes. We note that the flux ropes are a ubiquitous feature of the dayside ionosphere, occurring on every orbit down to the lowest altitudes.

C. T. RUSSELL
R. C. ELPHIC, J. A. SLAVIN
Institute of Geophysics and Planetary Physics, University of California, Los Angeles 90024

References and Notes

1. H. S. Bridge, A. J. Lazarus, C. W. Snyder, E. F. Smith, L. Davis, Jr., P. J. Coleman, Jr., D. E. Jones, *Science* **158**, 1669 (1967); N. F. Ness, K. W. Behannon, R. P. Lepping, Y. C. Whang, K. H. Schatten, *ibid.* **183**, 1301 (1974); Sh. Sh. Dolginov, Ye. G. Yeroshenko, L. Davis, *Kosm. Issled*, **7**, 747 (1969); Sh. Sh. Dilginov, Ye. G. Yeroshenko, L. N. Zhuzgov, V. B. Buzin, V. A. Sharova, *Pisma Astron. Zh* **2**, 8 (1976); K. I. Gringauz, V. V. Bezrukikh, G. I. Volkov, L. S. Musatov, T. K. Breus, *Kosm. Issled.* **8**, 431 (1970).
2. M. I. Verigin, K. I. Gringauz, T. Gombosi, T. K. Breus, V. V. Bezrukikh, A. P. Remizov, G. I. Volkov, *J. Geophys. Res.* **83**, 3721 (1978).
3. C. T. Russell, *ibid.* **82**, 625 (1977).
4. Sh. Sh. Dolginov, L. N. Zhuzgov, V. A. Sharova, V. B. Buzin, Ye. G. Yeroshenko, *Lunar Planet. Sci.* **9**, 256 (1978); C. T. Russell, *Geophys. Res. Lett.* **3**, 125 (1976); *ibid.*, p. 413; *ibid.*, p. 589.
5. For further details on the instrumentation, see R. C. Snare and J. D. Means, *IEEE Trans. Magn.* **MAG-13**, 1107 (1977).
6. J. H. Wolfe, H. Collard, J. D. Mihalov, and D. Intriligator provided solar wind measurements obtained with their plasma analyzer.
7. A. Nagy and L. Brace, personal communication.
8. E. W. Greenstadt, C. T. Russell, V. Formisano, P. C. Hedgecock, F. L. Scarf, M. Neugebauer, R. E. Holzer, *J. Geophys. Res.* **82**, 651 (1977).
9. We thank the entire Pioneer Venus team at Ames Research Center, Hughes Aircraft Company, and Westinghouse Corporation for successful fabrication, testing, and flight of the spacecraft and our instrument. At UCLA we are particularly indebted to R. C. Snare and J. D. Means for instrument design and testing and to N. Cline, M. Emig, and B. Litt for data analysis support. Supported by NASA contracts NAS 2-8088 and NAS 2-9491.

16 January 1979

Plasma Waves Near Venus: Initial Observations

Abstract. *The Pioneer Venus electric field detector observes significant effects of the interaction of the solar wind with the ionosphere of Venus all along the orbiter trajectory. Information is obtained on plasma oscillations emitted by suprathermal electrons beyond the bow shock, on sharp and diffuse shock structures, and on wave-particle interaction phenomena that are important near the boundary of the dayside ionosphere.*

Initial measurements by the electric field detector on the Pioneer Venus orbiter show that the solar wind interaction with the Venus ionosphere is strong and highly variable. Bursts of electron plasma oscillations are generally detected everywhere beyond the bow shock, indicating that suprathermal electrons are generated at the shock surface. In most cases the shocks themselves are well defined in terms of local generation of intense ion acoustic turbulence and whistler mode turbulence. The largest-amplitude plasma waves are frequently detected at very low altitudes in the neighborhood of the ionospheric boundary. In this region, a characteristic feature is the sharp onset of attenuation of the strong 100-Hz waves as the orbiter penetrates the dayside ionosphere. If this 100-Hz plasma wave turbulence represents whistler mode noise, damping of the waves by the ionospheric electrons can be an important interaction mechanism that transfers solar wind energy directly to the ionosphere.

The measurements of plasma wave activity near Venus are made by using a vee-type body-mounted electric dipole with an effective length of 0.7 m. This short antenna detects electric components of the waves in the spin plane, and the signals are processed in four independent bandpass channels having center frequencies at 100, 730, 5400, and 30,000 Hz. In each channel the bandwidth is 30 percent of the center frequency and the wave amplitude is continuously measured with an amplifier with automatic gain control. At the nominal spacecraft rate of 1024 bits per second, a four-channel spectral scan is transmitted every 1/2 second. This instrument was designed to provide exploratory information on all aspects of the solar wind interaction with Venus, and measurements are made throughout the orbit. The conclusions reported here are based on an analysis of quick-look data that include the 3-hour periods centered around periapsis for orbits 1 through 20; short samples of observations from all other parts of the orbits have also been examined.

Figure 1 shows summaries of the low-altitude observations for orbits 1 and 4. These measurements are typical for days with low solar activity and relatively high periapsis locations (380 km for orbit 1 and 180 km for orbit 4) on the dayside approaching the western (dusk) terminator. Peaks and averages of the wave spectral densities are shown along with preliminary magnetic field (B) profiles from the UCLA magnetometer and preliminary electron densities derived from the GSFC electron temperature probe. Bow shocks (near 1420 and 1625 on orbit 1) are clearly located by increases of B above the solar wind value; ionosphere boundaries (near 1508 and 1513 on orbit 1) are easily identified by increased electron densities and (generally) decreased B inside the ionosphere.

Since typical solar wind densities near Venus give plasma frequencies near 30 kHz, we identify the 30-kHz wave level enhancements detected beyond the bow shock as electron plasma oscillations generated by suprathermal electrons (*1*). Similar bursts are detected out to apoapsis, and the cutoff at the shock suggests that these electrons are generated at the shock surface. The wave measurements in the upstream solar wind and the observations of high levels of ion acoustic turbulence (5.4-kHz and 730-Hz channels) and whistler mode noise (100-Hz channel) at the inbound shocks on orbits 1 and 4 suggest that strong wave-particle interactions develop there. Mass loading by neutral atoms escaping from Venus into the upstream solar wind (*2*) does not appear important at these shock locations. However, the shocks encountered outbound on the same orbits are quite diffuse, with extensive upstream turbulence, and effects associated with mass loading by ions of atmospheric origin may influence the outbound shocks.

Figure 1 shows that some of the most interesting and novel results are found at very low altitudes. We very frequently observe the strongest wave bursts just outside the dense ionosphere; the 730-Hz peak at 1447 UT on 8 December 1978 (Fig. 1b) is one example. This peak and the rise in the 730-Hz average were detected near the outbound ionopause (*3*) on orbit 4. Strong currents must flow at this type of boundary, which separates the shocked and magnetized solar wind (hydrogen plasma) from the ionospheric heavy-ion plasma, and current-driven plasma instabilities can generate strong

 0036-8075/79/0223-0748$00.50/0